Sensors and Materials, Vol. 35, No. 1 (2023) 121–133
MYU Tokyo

S & M 3158

Remote Estimation of Suspended Matter Concentration in Hongze Lake, China Using the Experimental Tiangong-II Moderate-resolution Wide-wavelength Imager

Lin Hui,[1] Zeng Zhi,[2*] Du Chenggong,[3**] Pan Jinheng,[3]
Tian Yichao,[1] Yan Chen,[3] and Xie Xiaokui[1]

[1]College of Resources and Environment of Beibu Gulf University, Qinzhou, Guangxi 535011, China
[2]School of Computer Science and Engineering, Huizhou University, Huizhou, Guangdong 516007, China
[3]School of Life Sciences, Huaiyin Normal University, Huaiyin, Jiangsu 223300, China

(Received October 31, 2022; accepted January 19, 2023)

Keywords: moderate-resolution wide-wavelength images (MWI), Hongze Lake, total suspended particulate matter (TSPM), remote sensing

Total suspended particulate matter (TSPM) is an important indicator of water quality. Remote sensing has advantages of wide range and high time efficiency. The use of satellites to monitor TSPM concentration is of great significance for the study of water quality and eutrophication. Using the measured data on the ground and taking Hongze Lake as the research area, we compared and analyzed seven types of suspended particulate matter concentration estimation model based on Tiangong-II wide-band moderate-resolution wide-wavelength images (MWI), selected the TSPM concentration estimation model suitable for the MWI data of Hongze Lake, and verified the accuracy and applicability of MWI data products. The results show that the linear model constructed by using the band ratio combination of B5/B9 MWI data as a variable has a high estimation accuracy, with a determination coefficient of 0.94, an average absolute error percentage of 12.27%, and a root mean square error of 2.97 mg/L. Compared with the TSPM estimation results from the moderate-resolution imaging spectroradiometer data obtained on the same day, the two estimation results were similar, and the change trend of TSPM concentration is basically consistent. The TSPM concentration in Hongze Lake has an obvious spatial difference. Huaihe River Bay is affected by its inflow into the lake, and its TSPM concentration is the highest. The concentration in the east of the gulf of Lihe Bay was also affected by Huaihe River Bay. Owing to eutrophication, the TSPM concentration of Chengzi Bay is relatively high in some areas.

1. Introduction

With the development of the social economy and the increasing frequency of human activities, the eutrophication of inland water bodies is becoming increasingly severe, in

*Corresponding author: e-mail: zengzhi@hzu.edu.cn
**Corresponding author: e-mail: ducg1023@163.com
https://doi.org/10.18494/SAM4215

ISSN 0914-4935
https://myukk.org/

which the input of rivers brings in a large amount of suspended sediment, and nutrients from land-based sources are easily adsorbed in suspended particles into lakes, bringing a large number of nutrient salts to water bodies, which eventually leads to the eutrophication of water bodies and the outbreak of water wars.(1) In addition, the suspended matter itself affects the optical signal of inland water bodies and has an important impact on the growth of aquatic animals and plants, and the content of suspended matter in water has been used as an important indicator to measure the pollution level of water bodies and is included in the routine monitoring of water environment parameters. Hongze Lake, the fourth largest freshwater lake in China, is located in the northern part of Jiangsu Province, and there are numerous farmlands distributed around it with severe surface pollution. In addition, Huaihe River is the river with the largest flow into the lake and brings in a large amount of sediment every year. Moreover, the long-time sand mining activities in Hongze Lake also lead to the increase in its suspended matter concentration and further deterioration of water quality.(2) Therefore, the real-time and high-precision monitoring of suspended matter concentration in the water body of Hongze Lake is an important part of the current water quality management of the lake.

Unlike conventional water quality monitoring methods, remote sensing has the ability to monitor the lake water quality in real time, which can save time and effort and has a wide range.(3) As an optically active substance in water bodies, suspended particulate matter can be effectively monitored by remote sensing technology.(4) In addition, the remote sensing estimation of suspended matter concentration in inland water bodies has produced a series of research results, mainly divided into semi-analytical and empirical algorithms.(5–7) For multispectral data and specific study areas, the empirical method is simple and fast, and the estimation accuracy meets the needs of remote sensing monitoring. It is also more suitable for large-time-scale and large-data processing and applications.(8,9)

The Tiangong-II MWI sensor is an advanced experimental water color sensor designed for HY-1E and HY-1F satellites in China, and the MWI data are analyzed to ensure that the subsequent satellites can obtain high-quality water color information.(10,11) At present, there are corresponding models(12–14) for estimating suspended matter concentration for common water color sensors such as those based on MODIS, VIIRS, MERIS, and GOCI data, but there is a relative lack of research on estimating suspended matter concentration using MWI images, and there is no estimation of suspended matter concentration in Hongze Lake using MWI data. Therefore, in this study, we constructed and compared the accuracy and applicability of common models for estimating suspended matter concentration based on the measured data of Hongze Lake and selected the suitable model for estimating the suspended matter concentration in Hongze Lake using MWI data, to provide a reference for estimating the suspended matter concentration in inland water bodies using MWI data.

2. Data Collection and Processing

2.1 Study area

Hongze Lake, located between 33°06′ and 33°40′ N latitude and 118°10′ and 118°52′ E longitude, is a shallow and overwater lake in Jiangsu Province, which receives water from the upper and middle reaches of Huaihe River with a basin area of 158000 km^2, accounting for 83.6% of the Huaihe River basin. At the same time, it is also one of the main water transfer lines of the "South-to-North Water Transfer" East Project and a water transfer reservoir for water transfer. The rivers entering Hongze Lake are mainly in the west and south of the lake, and the volume of water from the Huaihe River accounts for more than 70% of the total water volume of the lake. The water body of Hongze Lake has complex optical characteristics and a high suspended sediment content, and is a typical class II water body, mainly divided into three lake bays with tremendous differences in water quality. Chengzi Lake Bay is relatively closed, with slow water exchange and a high degree of eutrophication; Huaihe River Bay is the overwater area of Hongze Lake, with intense lake flow disturbance and a high suspended sediment content; western Lihe Lake Bay is the main inlet river distribution area, with a strong self-purification ability of the water body, mainly distributed with aquatic grass and aquaculture. Its eutrophication degree is lower than that of Chengzi Lake, and in recent years, the water quality has begun to gradually deteriorate owing to the upstream discharge and sand mining activities.[9,13]

2.2 Water quality data sampling and analysis

A total of 27 sampling points were used for simultaneous water surface spectroscopy and water sample collection, and the distribution of sampling points is shown in Fig. 1. The water

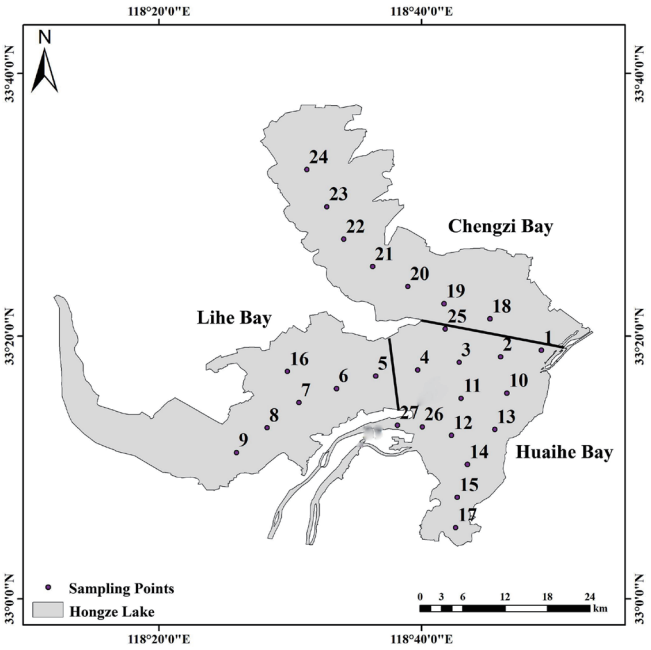

Fig. 1. Study area and distribution of sampling points.

samples were brought back to the laboratory on the day of the experiment, and the suspended matter content was measured using conventional measurement methods. The water surface spectral data were collected using an ASD Field Spec Pro portable spectrometer produced by ASD and converted to water surface remote sensing reflectance according to the method introduced by Cheng *et al.*[16]

2.3 TSPM estimation method

TSPM, as one of the three elements of water color, has a strong optical signal, so the remote sensing estimation of TSPM concentration has a high accuracy and it is a relatively mature method. The TSPM concentration of Hongze Lake is high and varies greatly in different lake areas, so it is urgent to find a TSPM estimation model for Hongze Lake applicable to MWI. TSPM remote sensing estimation models are mainly divided into empirical and semi-analytical models, and in this study, seven inversion models representative of inland water bodies were selected for comparative evaluation among the above two types of algorithm. They are the single-band, band-ratio, three-band, multiple regression, the SAI index method, the semi-analytical algorithm containing the 3S model, and the Nechad model.

Single-band, band-ratio, and multiple regression models are the main models currently used to construct TSPM remote sensing estimation models, mainly by analyzing the correlation between TSPM concentration and R_{rs} to find the optimal band or combination of bands, and then different mathematical models are used to determine the optimal estimation model. Multiple regression multiple optimal bands are independent variables for regression analysis to predict the dependent variable method. The three-band model uses $[R_{rs}(\lambda)_2 + R_{rs}(\lambda_3)]$ as the suspension sensitivity factor and $[R_{rs}(\lambda_1) + R_{rs}(\lambda_3)]$ as the chlorophyll sensitivity factor, and then we construct the form $TSPM = a + b[R_{rs}(\lambda_2) + R_{rs}(\lambda_3)] + c[R_{rs}(\lambda_1) / R_{rs}(\lambda_3)]$ as the suspension estimation model. Here, λ_1, λ_2, and λ_3 indicate three different wavelengths.

The SAI first requires the construction of a spectral index:

$$SAI = \frac{\left[d * R_{rs}(\lambda_1) + (1-d) * R_{rs}(\lambda_3)\right]}{R_{rs}\left(\lambda_2\right)}, \tag{1}$$

where $d = (\lambda_3 + \lambda_2) / (\lambda_3 + \lambda_{21})$, $\lambda_1\ \lambda_2\ \lambda_3$; a, b and c are constants.

The 3S semi-analytic algorithm considers that the TSPM can be estimated by applying the following equation:

$$TSPM = a + b\left[R_{rs}(\lambda_1)^{-1} - R_{rs}(\lambda_2)^{-1}\right]^{-1}, \tag{2}$$

where a and b are constant coefficients; λ_1 is between 690 and 900 nm; λ_2 is between 720 and 780 nm or 840 and 900 nm.

Then, a universal TSPM semi-analytical estimation method based on the bio-optical model was constructed as

$$TSPM = a\left[\frac{R_{rs}(\lambda)}{c - R_{rs}(\lambda)}\right] + b, \tag{3}$$

where a and b are constants and c is a constant with physical significance. A rate determination method has been developed for c using Class II water with a value of 0.093, and this value is adopted in this study.

2.4 Tiangong-II MWI data and preprocessing

MWI is an ocean water color sensor on board the Chinese space laboratory Tiangong-II, which is designed and studied mainly to meet the next generation of ocean satellites HY-1E and HY-1F to be able to monitor the water color information of ocean and coastal highly turbid water bodies with high performance and is suitable for carrying out inland lake monitoring as well as observing the water color and water temperature in the ocean and coastal zones. It is mainly composed of 14 bands, covering blue, green, red, and near-infrared. The spatial resolution is 100 m, which has excellent advantages compared with the rest of the water color sensors in ensuring more bands and also having a higher spatial resolution. Its specific band settings are shown in Table 1.

MWI data can be downloaded from the manned space application data promotion service platform (http://www.msadc.cn/sy/). In this study, we obtained cloud-free data from Hongze Lake on March 14, 2017. There is no perfect mature atmospheric correction method for MWI data. In this study, we used ENVI for flash atmospheric correction. This method has been widely applied to many sensors (e.g., Landsat and high-resolution series).[7,17,18]

2.5 Statistical analysis

In this study, two metrics, mean absolute percentage error (MAPE) and root mean square error (RMSE), are used to compare the accuracies of the models. The specific calculation steps are

Table 1
MWI band settings and parameter information.

Band	Band center (nm)	Pulse width (nm)	Spatial resolution (m)
B1	413	20	100
B2	443	20	100
B3	490	20	100
B4	520	20	100
B5	565	20	100
B6	620	20	100
B7	665	20	100
B8	682	20	100
B9	750	20	100
B10	820	20	100
B11	865	20	100
B12	905	20	100
B13	940	20	100
B14	980	20	100

$$MAPE = \frac{1}{n}\sum_{i=1}^{n}\left|\frac{y_i - y'_i}{y_i}\right| * 100\%, \tag{4}$$

$$RMSE = \sqrt{\frac{1}{n}\sum_{i=1}^{n}(y_i - y'_i)^2}. \tag{5}$$

Here, y_i and y'_i are the measured and simulated values, respectively, and n is the number of samples.

3. Results and Discussion

3.1 Analysis of water quality and optical properties of Hongze Lake

The concentrations of water quality parameters in 29 measured sample points uniformly distributed in Hongze Lake were statistically analyzed according to the partition shown in Fig. 1, and the results are shown in Table 2. The average suspended matter concentration in all sample points in the whole lake is 25.71 mg/L, and the concentrations in Huaihe River Bay and Chengzi Lake are higher, 27.98 and 27.93 mg/L, respectively, and 17.05 mg/L in Lihe Lake Bay, and the TSPM concentration is significantly lower than in the remaining two lakes. The TSPM in all three lakes and bays was dominated by inorganic suspended matter (ISM), and the concentration of ISM was about five times higher than that of organic suspended matter (OSM). According to Fig. 2, the fitting accuracy R^2 of TSPM and ISM concentrations reached 0.97, which was significantly higher than that of TSPM and OSM concentrations, further proving that ISM in Hongze Lake was an important component of TSPM. The chlorophyll a concentration was 12.84 μg/L, higher than those in Huaihe River Bay (9.71 μg/L) and Lihe Lake Bay (4.23 μg/L).

The remote sensing reflectance curves of the actual sampling sites are shown in Fig. 3. There is a reflectance peak at 575 nm, and then the remote sensing reflectance gradually decreases, and the changes in peak and trough are not obvious compared with those of algae-dominated water bodies, and there is no obvious spectral feature of algae water bodies. The spectral curve of Hongze Lake, which is a spectral curve dominated by ISM, is similar to the results of previous studies. In addition, the absorption coefficients of intrinsic optical quantity pigmented particles (a_{ph}) and non-pigmented particles (a_{nap}) were analyzed, and the absorption curve of pigmented particles had an absorption peak at 675 nm, whereas the absorption coefficient of non-pigmented particles showed an exponential decay. a_{ph} is dominant in TSPM and affects the concentration change of TSPM. Hongze Lake is a shallow inland lake dominated by suspended matter, with a

Table 2
Concentrations of water quality parameters in different lake areas of Hongze Lake.

Lake region	Mean TSPM (mg/L)	Mean ISM (mg/L)	Mean OSM (mg/L)	Mean Chl-a (μg/L)
Hongze Lake	25.71	20.99	4.71	9.32
Chengzi Lake	27.93	23.31	4.62	12.84
Huaihe River Bay	27.98	23.46	4.52	9.71
Lihe Lake Bay	17.05	11.71	5.33	4.23

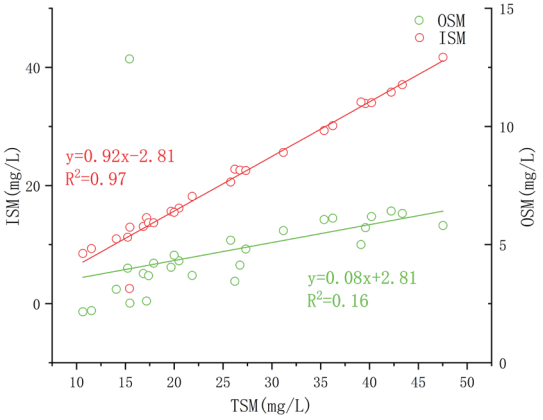

Fig. 2. (Color online) Characteristics of total suspended matter concentration in Hongze Lake.

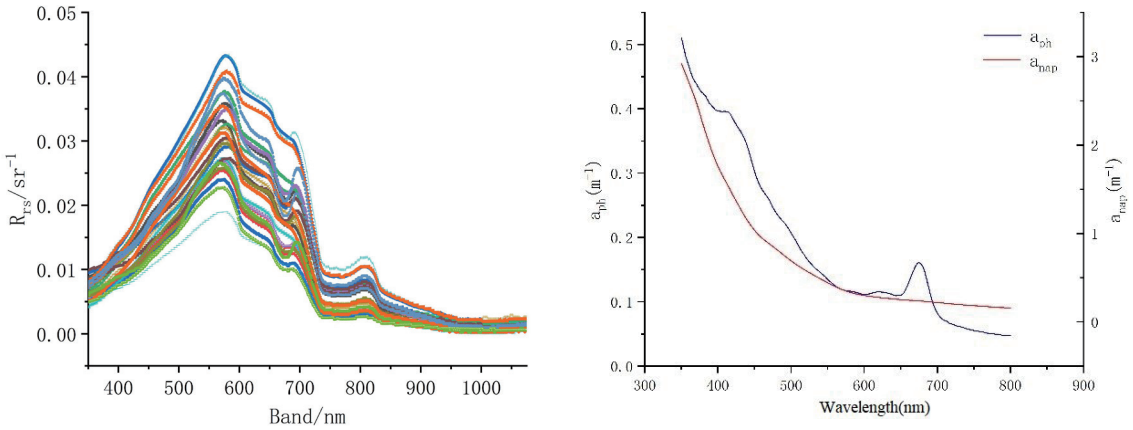

(a) (b)

Fig. 3. (Color online) (a) Measured remote sensing reflectance curve of Hongze Lake; (b) analysis of particle absorption characteristics of Hongze Lake.

fast water exchange cycle and susceptible to the effect of upstream water from Huaihe River and meteorological factors, and its suspended matter is mostly sediment.

3.2 MWI-based TSPM remote sensing estimation model construction

In this study, firstly, the measured spectral data are simulated to 14 bands of the Tiangong-II MWI sensor according to the MWI spectral response function, and the ground 27 measured sample data are divided into the modeling and validation data sets, 20 sample points of which are modeled and 7 sample points are validated. The optimal waveband position of the model was determined by correlation analysis, and the results of single-band and combined-band correlation analyses are shown in Fig. 4. The single-band correlation coefficients range from 0.51 to 0.91,

indicating that the overall trend of remote sensing reflectance increases with the suspended matter concentration. The maximum correlation coefficient is 0.91, which is located in the 9th band of the Tiangong-II MWI sensor. The center wavelength of this band is 750 nm, which belongs to the near-infrared band, and the correlation coefficients at B10, B11, and B12 are also higher, which are 0.89, 0.87, and 0.81, respectively, indicating that the remote sensing reflectance from 750 to 900 nm can be used to estimate the TSPM concentration of water bodies. The correlation between the band ratio combination and the TSPM concentration fluctuates widely, with coefficients ranging from −0.92 to 0.69. The band ratio combined with the highest correlation is B5/B9, with a correlation coefficient of −0.92, so this band combination will be selected for the construction of the band ratio algorithm.

In addition, the seven algorithms introduced in Sect. 2.3 were used for the estimation of TSPM concentration, and the results are shown in Table 3. It can be seen that all types of model constructed on the basis of ground truth data have good accuracy, and the band ratio model has the highest accuracy with MAPE and RMSE of 10.82% and 2.04 mg/L, respectively, followed by the single-band model, and the less accurate are the 3S and three-band models. The reason for the low accuracy of the semi-analytical model may be that the training data used in the model construction are not collected from Hongze Lake, which leads to the model accuracy being affected; the reason for the low accuracy of the three-band model is that Hongze Lake is mainly a highly turbid water body dominated by suspended matter, which is less affected by chlorophyll a. The key parameters are not re-rated, which leads to the low accuracy of the algorithm. The parameter c in the Nechad model is based on the data of the Yangtze River estuary. Therefore, it is necessary to further determine the intrinsic optical quantities for the water bodies of Hongze Lake, re-rate these parameters, and construct a semi-analytical method suitable for the water bodies of Hongze Lake.

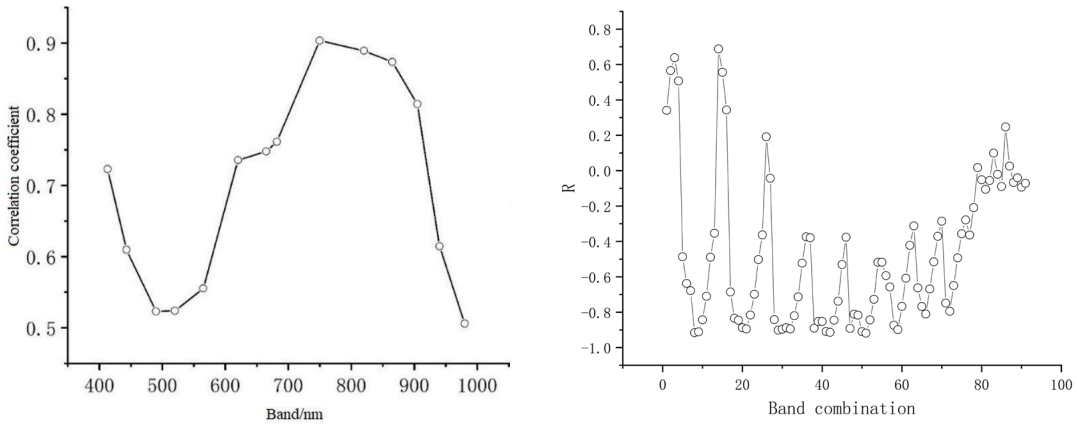

(a) (b)

Fig. 4. (a) Correlation coefficient between TSPM and R_{rs} at different wavelength bands; (b) correlation coefficient between TSPM and R_{rs} at different wavelength band combination factors.

Table 3
Various optimal inversion models based on measured data and their accuracy evaluation.

Model (algorithm)	Formula	Band	R^2	*MAPE* (%)	*RMSE* (mg/L)
Single band	$TSPM = 4538.4x + 1.32$	B(750)	0.91	12.27	2.97
Band ratio	$TSPM = 1.31x^2 - 23.08x + 115.73$	B(565)/B(750)	0.94	10.82	2.04
Three bands	$\mathrm{Log}_{10}(TSPM) = 1.21 + 11.85x1 - 0.65x2$	B(490),B(565),B(665)	0.54	19.88	8.98
SAI index	$\mathrm{Log}_{10}(TSPM) = 3.73SAI + 0.71$	B(490),B(565),B(750)	0.89	11.96	2.76
Multiple regression	$TSPM = 20.15 + 6531.17x1 - 1187.25x2$	B(520),B(750)	0.90	13.15	3.53
3S	$TSPM = -3263.1x + 5.56$	$[B(820)^{-1} - B(865)^{-1}]^{-1}$	0.68	31.42	27.35
Nechad	$TSPM = 326.64x + 4.49$	B(820)/[0.093−B(820)]	0.79	13.41	5.50

3.3 Evaluation of the applicability of the model

To analyze the applicability of the above TSPM concentration remote sensing model in Hongze Lake, the estimation accuracy of the model was further analyzed at different TSPM concentrations. According to the measured TSPM concentration range in Hongze Lake, the obtained TSPM concentrations were divided into two categories, namely, less than 25 mg/L and more than 25 mg/L. The TSPM remote sensing estimation models applicable to different categories were constructed by using the above seven models, and the results are shown in Table 4. In the TSPM concentration category of less than 25 mg/L, the band ratio model has the highest accuracy with the lowest MAPE of 11.34%, and the 3S model has the lowest accuracy with the MAPE of 21.91%; in the TSPM concentration category of greater than 25 mg/L, the multiple regression model has the highest accuracy with the MAPE of 2.81%, followed by the better band ratio model and the SAI index model. A comparison of the modeling accuracies of the models in different TSPM concentration categories showed that the modeling accuracy of the empirical algorithm was significantly higher than that of the semi-analytical algorithm, in which the band ratio model performed stably and had a higher accuracy in both categories. Therefore, the band ratio model is considered to be the most suitable for estimating the TSPM concentration in Hongze Lake.

In summary, for inland turbid water bodies, the empirical model for the remote sensing estimation of TSPM concentration has a high accuracy, mainly because the suspended particles in the lake contain all insoluble solid particles including algal particles, which generate an optical signal. This optical signal is more obvious and less disturbed than that generated by the remaining two optically active substances. When the suspended particulate matter concentration increases, the backscattering signal will be strengthened and the remote sensing reflectance will generally become higher. In particular, the remote sensing reflectance changes in the near-infrared band are more sensitive to the changes in TSPM concentration, and it is the band that is commonly adopted for TSPM concentration estimation, such as in the Dongting Lake and Poyang Lake areas, which are also dominated by suspended matter. Zheng *et al.*[19] and Gao *et al.*[20] constructed high-precision remote sensing estimation models of suspended matter concentration using NIR bands applicable to their respective study areas. They showed that the

Table 4
Accuracy evaluation of TSPM in Hongze Lake at different TSPM concentrations.

Model	*TSPM* ≤ 25mg/L		*TSPM* ≥ 25mg/L	
	MAPE (%)	*RMSE* (mg/L)	*MAPE* (%)	*RMSE* (mg/L)
Single band	11.52	1.94	14.61	6.53
Band ratio	11.34	1.87	3.71	1.42
Three bands	12.94	2.31	16.62	6.86
SAI index	16.37	3.04	3.51	1.10
Multiple regression	12.12	2.08	2.81	1.06
3S	21.91	3.84	21.04	7.79
Nechad	12.84	2.10	15.54	6.77

remote sensing estimation model of suspended sediment concentration using NIR bands is feasible and has some generalization. Therefore, the empirical models constructed on the basis of these characteristic wavebands have a high accuracy and can meet the application requirements.

To evaluate further the applicability of MWI data for estimating the concentration of suspended solids in Hongze Lake, MODIS and MWI data were selected for comparison and analysis, and the signal-to-noise ratios of the two sensors were first compared. The signal-to-noise ratio of MODIS data is significantly higher than that of MWI data, partly owing to the spatial resolution; the higher the spatial resolution, the lower the signal-to-noise ratio,[10] and the spatial resolution of MODIS is 1 km, whereas that of MWI can reach a length of 100 m, which is an advantage that MODIS data does not have.

We select the MODIS and MWI data obtained on the same day for TSPM concentration estimation, and the MODIS estimation model was adopted from previous studies[2] to compare the estimation results of the two images on the same day and explore whether the difference in signal-to-noise ratio would have a greater impact on the results of TSPM concentration estimation from the MWI data. According to Fig. 5, the results of the two images are the same, and the TSPM concentrations and variation trends are also the same. It is worth noting that, because of the higher spatial resolution of MWI, the distribution characteristics of the TSPM concentration shown are more obvious and better reflect the detailed information.

3.4 Spatial distribution of suspended matter concentrations in Hongze Lake based on Tiangong-II MWI data

The constructed model was applied to the atmospherically corrected Tiangong-II MWI images to obtain the spatial distribution of TSPM concentration in Hongze Lake on March 14, 2017, as shown in Fig. 6. The TSPM concentration in Huaihe River Bay is significantly higher than those in the other two bays, and the TSPM concentration in Lihe Lake Bay is higher near the Huaihe River inlet area. In addition, the TSPM concentration in the Xihu Lake area is lower, and the TSPM concentration in Chengzi Lake Bay is also higher than that in Huaihe River Bay. In addition, the TSPM concentration gradually decreases from the Huaihe River inlet river mouth to Huaihe River Bay, and there is an obvious trend of diffusion.

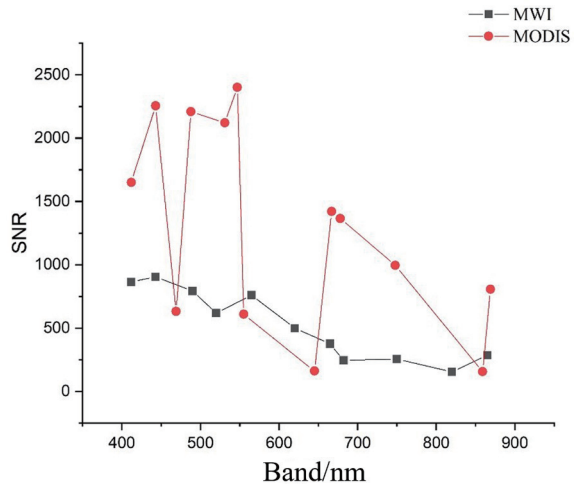

Fig. 5. (Color online) Comparison of signal-to-noise ratio between MWI and MODIS data.

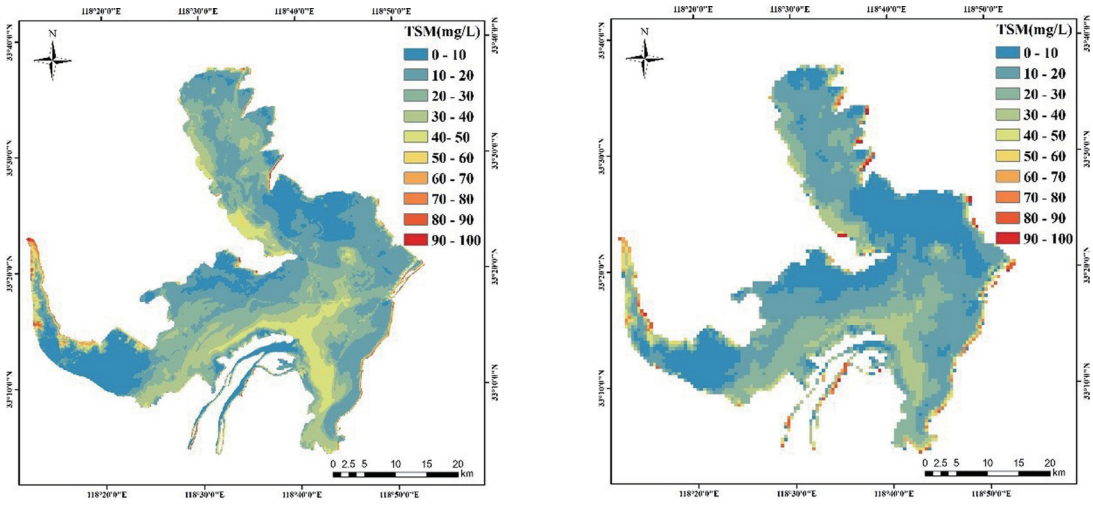

(a) (b)

Fig. 6. (Color online) Results of TSPM concentration in Hongze Lake estimated from MWI and MODIS data obtained on March 14, 2017.

Huaihe River is the largest river flowing into Hongze Lake, and a large number of pollutants from the Huaihe River basin are transported to Hongze Lake through Huaihe River, so the TSPM concentration is highest at the Huaihe River estuary and gradually decreases as the distance from the estuary increases with the diffusion effect of water flow. Huaihe River Bay is susceptible to the wind speed and churning caused by cargo ships because the lake is open and navigable,[21] and the TSPM concentrations are also higher. Chengzi Lake Bay does not have large inlet rivers and is less polluted by surface sources. In addition, because this lake bay is narrow and long, it is also weakly affected by meteorological factors such as wind speed, so its TSPM concentration is lower than that of Huaihe River Bay. The eastern area of Lihe Lake Bay is affected by the entry of Huaihe River into the lake, so the TSPM concentration is higher, whereas the western area is less affected, so the concentration is lower.

We adopted the method of optimized APF upon DRL to solve the problem of global path planning caused by the local optimal solution of the APF method, which introduces the unique reward and punishment function of RL.

4. Conclusion

In this study, the remote sensing estimation of TSPM concentration in Hongze Lake was investigated by using the field experiment sampling data of Hongze Lake and the MWI data of Tiangong-II. The results show that the waveband ratio algorithm (B5/B9) has good model accuracy and stability, and the estimation results from MWI data are compared with those from MODIS data. Although the signal-to-noise ratio of MWI data is lower than that of MODIS data, the optical signal of suspended particulate matter in the inland highly turbid water body is lower than that of MODIS. The optical signal of suspended particulate matter is stronger, and the estimation results of both images are similar to those of MODIS, indicating that the estimation results of MWI images can meet the needs of the remote sensing estimation study of TSPM concentration in Hongze Lake.

In addition, by using the Tiangong-II data obtained on March 14, 2017 to estimate the TSPM concentration in Hongze Lake, the MWI data can clearly show the spatial distribution of the TSPM concentration in Hongze Lake, reflecting the variation in TSPM concentration due to the effect of external factors such as wind direction. From the spatial distribution, owing to the effect of the Huaihe River inlet river, the TSPM concentration in the Huaihe River inlet estuary is significantly higher than in the rest of the region. The TSPM concentration from the estuary to Huaihe River Bay shows a gradually decreasing trend, and that in Huaihe River Bay is also higher owing to the effect of the resuspension of the bottom sediment caused by navigation. The TSPM concentrations in the Chengzi Lake Bay and Lihe Lake Bay regions are relatively lower.

The MWI data from Tiangong-II in this study has achieved good applicability for TSPM concentration estimation in Hongze Lake, providing new data source and method for water environmental protection in Hongze Lake, which can be extended and applied to the remote sensing estimation study of TSPM concentration in other similar turbid water bodies in the future. It is also necessary to further collect ground-based synchronous data to obtain the measured data covering different seasons to further verify the applicability of the TSPM estimation model.

Acknowledgments

We would like to express our sincere thanks to the Manned Space Program for providing the Tiangong-II Wide-Band Imager data products. This study was jointly supported by the National Natural Science Foundation of China (42001296), Natural Science Foundation of Jiangsu Province (BK20191058), Natural Science Research Project of Colleges and Universities of Jiangsu Province (19KJB170001), Social Development of Key R&D Program of Jiangsu Province -- Major Science and Technology Demonstration Project (BE2018678), the key projects of

Guangdong Provincial Department of Education (2022ZDZX3030), Beibu Gulf University High-level Talents Research Start-up Fund Project (2021KYQD03), and Marine Science Guangxi First-Class Subject, Beibu Gulf University (DTA004).

References

1 B. Q. Qin, L. Y. Yang, F. Z. Chen, G. W. Zhu, L. Zhang, and Y. Chen: Chin. Sci. Bull. **51** (2006) 1857.
2 Z. Cao, H. Duan, L. Feng, R. Ma, and K. Xue: Remote Sens. Environ. **192** (2017) 98.
3 W. Qu, Z. G. Pang, T. J. Lei, W. L. Song, J. X. Lu, K.Yang, and Y. N. Tang: Water Resour. Hydropower Eng. **52** (2021) 23. http://doi.org/10.13928/j.cnki.wrahe.2021.07.003
4 G. Zheng and P. M. Digiacomo: Prog. Oceanogr. **159** (2017) 45. http://doi.org/10.1016/j.pocean.2017.08.007
5 F. K. Ma, Z. B. Gao, and B. L. Ye: Water Resour. Dev. Manage. **5** (2021) 69. http://doi.org/10.1016/j.cnki.10-1326/TV.2021.05.15
6 J. Chen, W. Quan, Z. Weng, and T. Cui: Environ. Earth Sci. **69** (2013) 2709. https://doi.org/10.1007/s12665-012-2093-1
7 A. A. Gitelson, D. Gurlin, W. J. Moses, and T. Barrow: Environ. Res. Lett. (2009). https://doi.org/10.1088/1748-9326/4/4/045003
8 K. Shi, Y. Zhang, G. Zhu, X. Liu, Y. Zhou, H. Xu, B. Qin, G. Liu, and Y. Li: Remote Sens. Environ. **164** (2015) 43. https://doi.org/10.1016/j.rse.2015.02.029
9 Z. Zhang, Y. Li, Y. Guo: Remote Sens.-Basel. **7** (2015) 13975. https://doi.org/10.3390/rs71013975
10 Z. Cao, H. Duan, Q. Song, M. Shen, R. Ma, and D. Liu: Int. J. Appl. Earth Obs. **71** (2018) 109. https://doi.org/10.1016/j.jag.2018.05.012
11 J. Li, L. Tian, and Q. Song: IEEE J. Sel. Top. Appl. Earth Obs. Remote Sens. **3** (2019) 1. https://doi.org/10.1109/JSTARS.2019.2896729
12 Y. Wei, B. Matsushita, C. Jin, and T. Fukushima: Remote Sens. Environ. **115** (2011) 1247. https://doi.org/10.1016/j.rse.2011.01.007
13 C. Huang, Y. Li, Q. Wang, H. Lv, and D. Sun: J. Infrared Millimeter Waves **32** (2013):462. https://doi.org/10.3724/SP.J.1010.2013.00462
14 M. Marghany and M. Hashim: Int. J. Phys. Sci. **5** (2010) 1489. https://doi.org/10.3174/ajnr.A1518
15 J. Wang, Y. Zhang, F. Yang, X. Cao, Z. Bai, J. Zhu, E. Chen, Y. Li, and Y. Ran: J. Environ. Earth Sci. **73** (2015) 4063. https://doi.org/10.1007/s12665-014-3691-x
16 H. Cheng, C. Lin, L. Wang, J. Xiong, and C. Zhu: Int. J. Environ. Res. Public Health. **17** (2020) 1790. https://doi.org/10.3390/ijerph17051790
17 Q. I. Ling, J. Huang, J. Gao, Q. Huang, Y. Zhou, and W. Tian: J. Lake Sci. **28** (2016) 583. https://doi.org/10.18307/2016.0314
18 J. Tang, G. Tian, X. Wang, X. Wang, and Q. Song: J. Remote Sens. **8** (2004) 37.
19 Z. Zheng, J. Ren, Y. Li, C. Huang, L. Ge, C. Du, and H. Lv: Sci. Total Environ. **573** (2016) 39. https://doi.org/10.1016/j.scitotenv.2016.08.019
20 C. Gao, J. Xu, D. Gao, L. Wang, and Y.Wang: Remote Sens. Land Resour. **31** (2019) 101. https://doi.org/10.6046/gtzyyg.2019.01.14
21 S. Lei, D. Wu, Y. Li, Q. Wang, C. Huang, and G. Liu, Z. Zheng, C. Du, M. Mu, J. Xu, and H. Lv: Int. J. Remote Sens. **40** (2018) 3179. https://doi.org/10.1080/01431161.2018.1541109